Asia Pac. J. Math. 2026 **13**:32

ENHANCING IMAGE RESOLUTION BY MINIMIZING SALT-AND-PEPPER NOISE USING A NOVEL CONJUGATE GRADIENT APPROACH

BASIM A. HASSAN[1], TALAL ALHARBI[2,*]

[1]Department of Mathematics, College of Computers Sciences and Mathematics, University of Mosul, Iraq

[2]Department of Mathematic, College of Science, Qassim University, Buraydah 52571, Saudi Arabia

[*]Corresponding author: Ta.alharbi@qu.edu.sa

Received Jan. 9, 2026

Abstract. Image recovery is a pressing problem in recovering high-quality corrupted images by noise and distortion, especially salt-and-pepper noise, which severely degrades visual definition. This paper introduces an enhanced conjugate gradient (CG) approach, the BBS algorithm, to effectively restore images. The proposed method is a two-stage approach: an adaptive median filter detects and isolates noisy pixels in stage one, and a nonsmooth optimization problem is formulated in stage two in order to restore the corrupted pixels. To tackle computational challenges, the problem is reformulated as a smooth optimization problem, which is solved via the BBS algorithm, which employs a new parameter that emerges from Taylor series approximations. The BBS algorithm is also found to be computationally quicker than the normal Fletcher-Reeves (FR) algorithm, as can be demonstrated by numerical experiments conducted on typical test images (e.g., Lena, House, Elaine, Cameraman). The outcomes indicate faster rates of convergence, smaller iterations (NI), smaller function evaluations (NF), and better peak signal-to-noise ratios (PSNR). Performance profiling also attests to the performance of BBS, with the curves of the former significantly outperforming FR in iteration counts and computationally. Global convergence of the BBS algorithm under conditions of descent and Lipschitz continuity is demonstrated through theoretical analysis. The BBS algorithm is established as a computationally effective and robust image restoration method by this work and represents important improvements over the conventional CG methods of salt-and-pepper noise handling.

2020 Mathematics Subject Classification. 65K05; 90C06; 90C30; 90C47; 90C90.

Key Words: optimization problems; image restoration; two-phase approach; nonsmooth optimization; conjugate gradient (CG) method and convergence.

1. Introduction

Image restoration pertains to the systematic endeavor of reconstructing a compromised image by alleviating the influences of noise, blurring, and various modalities of distortion. The principal aim is

DOI: 10.28924/APJM/13-32

to recuperate the original image with exemplary fidelity through the processes of noise attenuation, distortion rectification, and enhancement of details. In the present investigation, the proposed conjugate gradient algorithm is utilized to tackle the complexities associated with image restoration [1–3].

In [2], authors proposed a bifurcated methodology designed to restore images that have been tainted by impulse noise, during the preliminary phase, a median filter was employed to identify and segregate pixels affected by noise. Consider an image X characterized by dimensions $M \times N$, wherein the spatial coordinates of each pixel are delineated by the index set $A = \{1, 2, \ldots, M\} \times \{1, 2, \ldots, N\}$ [4,5]. Let $|N|$ signify the count of pixels identified as compromised by noise during the preliminary detection phase, and let $N \subset A$ denote the subset of indices that correspond to these pixels affected by noise. For any pixel situated at coordinates $(m, n) \in A$, the collection of its four immediate neighboring pixels is represented by B_{mn}. Additionally, let $y_{m,n}$ denote the observed intensity value at the pixel location (m, n). In the subsequent phase of the restoration process, the recovery of the pixels deemed corrupted is formulated as a nonsmooth optimization problem [6], which seeks to precisely reconstruct the original intensities of the pixels:

$$\min_{q} \sum_{(m,n)\in N} \left[|q_{m,n} - y_{m,n}| + \frac{\beta}{2}(2 \cdot Z^1_{m,n} + Z^2_{m,n}) \right], \tag{1}$$

where:

$$Z^1_{m,n} = \sum_{(a,b)\in B_{m,n}} \psi_\alpha(q_{m,n} - y_{a,b}), \quad Z^2_{m,n} = \sum_{(a,b)\in B_{m,n}\setminus N} \psi_\alpha(q_{m,n} - q_{a,b}). \tag{2}$$

The function, $\psi_\alpha(t) = \sqrt{t^2 + \alpha}$, where $\alpha > 0$ is a parameter, operates as a term for regularization that preserves edges [4,7]. This function holds particular significance for tasks pertaining to noise elimination that endeavor to retain essential features of the image [4], such as edges. The vector $q = [q_{m,n}]_{(m,n)\in N}$ is characterized as a column vector based on length, with the set $|N|$ arranged in a lexicographic sequence. Resolving the nonsmooth minimization problem delineated in equation (1) with precision necessitates considerable computational resources and time. To mitigate this issue, Chan et al. [5] proposed a technique that removes the nonsmooth term, thereby yielding the subsequent smooth and unconstrained optimization problem:

$$\min_{q} f_\alpha(q) := \sum_{(m,n)\in N} \left(2 \sum_{(a,b)\in B_{m,n}\setminus N} \psi_\alpha(q_{m,n} - y_{a,b}) + \sum_{(a,b)\in B_{m,n}\cap N} \psi_\alpha(q_{m,n} - q_{a,b}) \right). \tag{3}$$

The intricacy of problem (3) escalates in direct correlation with the level of noise present. By utilizing the Conjugate Gradient (CG) method to address the optimization problem (3), the researchers in [8] exhibited a proficient restoration of images that had been compromised. In the current investigation, salt-and-pepper noise, which represents a distinct category of impulse noise, is tackled through a two-phase methodology [17]. In the initial phase, the identification of noisy pixels is conducted utilizing

an adaptive median filter as elucidated in [4]. Following this, problem (3) is resolved employing the proposed BBS algorithms [9], with its efficacy being compared to the FR method.

Conjugate gradient algorithms repeatedly compute the new point x_{k+1} using the current point x_k and a search direction d_k that is conjugate to the past directions [10]. This is the standard update guideline:

$$x_{k+1} = x_k + \alpha_k d_k, \tag{4}$$

where the step size, denoted by α_k, is as follows:

$$\alpha_k = -g_k^T d_k / d_k^T G d_k, \tag{5}$$

see [11]. The Wolfe criteria are satisfied by a line search approach that is commonly used to find α_k, as:

$$f(x_k + \alpha_k d_k) \leq f(x_k) + \delta \cdot \alpha_k g_k^T d_k, \tag{6}$$

$$d_k^T g(x_k + \alpha_k d_k) \geq \sigma \cdot d_k^T g_k, \tag{7}$$

where $0 < \delta < \sigma < 1$ [12]. The conjugate direction, d_k is updated as follows:

$$d_{k+1} = -g_{k+1} + \beta_k \cdot d_k. \tag{8}$$

The gradient of the objective function at iteration $k+1$ is denoted by g_{k+1}, whereas the amount of the previous direction that is preserved in the current iteration is determined by β_k, a scalar. The Fletcher-Reeves (FR) [13] formula is among the most widely used formulas for calculating β_k, as:

$$\beta_k^{FR} = \frac{g_{k+1}^T g_{k+1}}{g_k^T g_k}. \tag{9}$$

Faster convergence than straightforward steepest descent techniques is achieved by using this formula, which guarantees that the directions stay conjugate with respect to the Hessian matrix (in the case of quadratic functions). The conjugate gradient approach works particularly well for large-scale issues when it is not feasible to save or invert the Hessian matrix [11]. This makes it an extremely useful mathematical tool.

2. New parameter derived from the Taylor series

To derive the new conjugate gradient parameter, it is essential to understand the Taylor series thoroughly [9]. Let us proceed step by step:

$$f_k = f_{k+1} - g_{k+1}^T s_k + \frac{1}{2} s_k^T Q(x_{k+1}) s_k, \tag{10}$$

For this function, the gradient is defined as follows:

$$g_{k+1} = g_k + Q(x_{k+1}) s_k. \tag{11}$$

By combining equations (10) and (11), the second-order curvature is derived as follows:

$$s_k^T Q(x_{k+1}) s_k = \frac{3}{2} s_k^T y_k + (f_{k+1} - f_k), \tag{12}$$

where $y_k = g_{k+1} - g_k$. Through algebraic manipulation, we can deduce that:

$$s_k^T Q(x_k) s_k = \frac{3}{2} \frac{(g_k^T s_k)^2}{s_k^T y_k + (f_k - f_{k+1})} = \varpi_k s_k^T y_k, \tag{13}$$

where:

$$\varpi_k^1 = \frac{3}{2} \frac{(g_k^T s_k)^2}{s_k^T y_k (s_k^T y_k + (f_k - f_{k+1}))}. \tag{14}$$

Therefore, the expression for the matrix $Q(x_k)$ can be written as:

$$Q(x_k) = \frac{\varpi_k s_k^T y_k}{s_k^T s_k} I_n, \tag{15}$$

where I_n denotes the identity matrix. Substituting equation (15) into the conjugacy condition yields the following result:

$$\beta_k = \left(1 - \frac{s_k^T s_k}{\varpi_k s_k^T y_k}\right) \frac{g_{k+1}^T s_k}{s_k^T s_k}. \tag{16}$$

Employing the formula above, the expression becomes:

$$\beta_k^{BBS} = \frac{1}{s_k^T s_k} \left(y_k - \frac{1}{\varpi_k} s_k\right)^T g_{k+1}. \tag{17}$$

Equation (17) results from applying an exact line search to equation (14), yielding a more refined expression:

$$\varpi_k^2 = \frac{3}{2} \frac{(g_k^T s_k)^2}{s_k^T s_k (-s_k^T g_k + (f_k - f_{k+1}))}, \tag{18}$$

and

$$\varpi_k^3 = \frac{3}{2} \frac{(g_k^T s_k)^2}{s_k^T s_k (\alpha_k \|g_k\|^2 + (f_k - f_{k+1}))}. \tag{19}$$

For the sake of simplicity, we refer to these methods as BBS1, BBS2, and BBS3. They are referred to as BBS for convenience.

Algorithm BBS:. **Input:** To minimize a function by adjusting $x_0 \in \mathbb{R}^n$, ε.

Output: Find the optimal x with near-zero gradient.

(1) If $\|g_k\| < \varepsilon$ stop.

(2) Calculate α_k using (6) and (7).

(3) Obtain $x_{k+1} = x_k + \alpha_k d_k$.

(4) Calculate β_k by (17) and use in $d_{k+1} = -g_{k+1} + \beta_k d_k$.

(5) Set $k = k + 1$ and return to step 2.

3. Convergence analysis

The investigation into the global convergence of BBS algorithms constitutes the subsequent area of interest [18]. The ensuing premise is established:

Define the set $L_0 = \{x \in \mathbb{R}^n : f(x) \leq f(x_0)\}$. This set is assumed to be convex [6]. Furthermore, the gradient of the function f satisfies a Lipschitz continuity condition on L_0. Specifically, there exists a positive constant $L > 0$ such that for every pair $\bar{\sigma}$, and v^+ in L_0, the following holds:

$$\|\nabla f(\bar{\sigma}) - \nabla f(v^+)\| \leq L\|\bar{\sigma} - v^+\|. \tag{20}$$

Under these premises, it follows that there exists a constant $\Pi > 0$ that bounds the magnitude of the gradient at iteration $k + 1$:

$$\|g_{k+1}\| \leq \Pi. \tag{21}$$

Theorem 1. If d_{k+1} is descent, then $s_k^T y_k \neq 0$ and the search directions generated by (8) and (17) are descent directions.

Proof: We obtain $g_0^T d_0 = -\|g_0\|^2 < 0$ since $d_0 = -g_0$. Let $d_k^T g_k \leq 0$ be true.

By multiplying by g_{k+1}, we obtain:

$$d_{k+1}^T g_{k+1} = -\|g_{k+1}\|^2 + \left(1 - \frac{s_k^T s_k}{\varpi_k s_k^T y_k}\right) \frac{y_k^T g_{k+1}}{s_k^T y_k} s_k^T g_{k+1}. \tag{22}$$

It is clear from $s_k = \alpha_k d_k$, that:

$$d_{k+1}^T g_{k+1} = -\|g_{k+1}\|^2 + \left(\frac{\varpi_k s_k^T y_k - s_k^T s_k}{\varpi_k s_k^T y_k}\right) \frac{y_k^T g_{k+1}}{s_k^T y_k} s_k^T g_{k+1}. \tag{23}$$

Applying the Lipschitz condition yields the following results: $y_k^T g_{k+1} \leq L s_k^T g_{k+1}$ and $s_k^T y_k \leq L s_k^T s_k$. This enables us to write:

$$d_{k+1}^T g_{k+1} \leq -\|g_{k+1}\|^2 + \left(\frac{\varpi_k L s_k^T s_k - s_k^T s_k}{\varpi_k s_k^T y_k}\right) \frac{L(s_k^T g_{k+1})^2}{s_k^T y_k}. \tag{24}$$

However, because L is small and α_k^2 is very small, take notice of:

$$d_{k+1}^T g_{k+1} \leq 0. \tag{25}$$

The theorem is proven.

Dai et al. [20] show the general result in the following way for any conjugate gradient technique utilising the Wolfe line search. Also, extensions of this analysis appear in [12, 19].

Lemma 1. Any conjugate gradient technique (4) with $d_{k+1} = -g_{k+1} + \beta_k d_k$ as a descent direction, as found by the strong Wolfe line search, should be taken into consideration if assumptions (i) and (ii) are true. If:

$$\sum_{k\geq 1} \frac{1}{\|d_k\|^2} = \infty, \tag{26}$$

then

$$\lim_{k\to\infty} \inf \|g_k\| = 0. \tag{27}$$

One may use Lemma 1 to demonstrate the following conclusion.

Theorem 2. If a constant $\mu > 0$ exists such that, for every k, it satisfies:

$$(\nabla f(u) - \nabla f(w))^T (u - w) \geq \mu \|u - w\|^2, \quad \forall u, w \in \mathbb{R}^n, \tag{28}$$

based on Lemma 1's presumptions, we have:

$$\lim_{k\to\infty} \inf \|g_k\| = 0. \tag{29}$$

Proof: From (17), it is evident that:

$$\|d_{k+1}\| = \|g_{k+1}\| + \left|(1-\omega)\frac{g_{k+1}^T y_k}{s_k^T y_k}\right| \|s_k\|, \tag{30}$$

where $\omega = s_k^T s_k / (\varpi_k s_k^T y_k)$. It is clear from using Cauchy's inequality that:

$$\begin{aligned} \|d_{k+1}\| &\leq \|g_{k+1}\| + |1-\omega| \frac{\|g_{k+1}\|\|y_k\|}{\|s_k\|\|y_k\|} \|s_k\| \\ &\leq (2-\omega)\|g_{k+1}\|. \end{aligned} \tag{31}$$

Therefore, $\|\nabla f(x)\| \leq \Gamma$ implies that:

$$\sum_{k\geq 1} \frac{1}{\|d_k\|^2} \geq \left(\frac{1}{2-\omega}\right)^2 \frac{1}{\Gamma^2} \sum_{k\geq 1} 1 = \infty. \tag{32}$$

It follows that $\lim_{k\to\infty} \inf \|g_k\| = 0$ utilizing Lemma 1 [20–22].

4. Numerical results

We present some numerical data in this section to demonstrate the effectiveness of the new method in eliminating salt-and-pepper impulse noise. We evaluate the BBS and FR approaches in our experiments. Every code has been written in MATLAB r2017a. Then, a PC runs them. The halting requirements for both approaches are as follows:

$$\frac{|f(x_k) - f(x_{k-1})|}{|f(x_k)|} \leq 10^{-4} \quad \text{and} \quad \|\nabla f(x_k)\| \leq 10^{-4}(1 + |f(x_k)|). \tag{33}$$

Along with the test text, the test images feature Lena, House, Elaine, and the cameraman. Similar to [8], we qualitatively assess the restoration performance using the PSNR (peak signal to noise ratio) [23,26], which is defined as follows:

$$\text{PSNR} = 10\log_{10}\frac{255^2}{\frac{1}{MN}\sum_{i,j}(u^r_{i,j}-u^*_{i,j})^2}, \tag{34}$$

where $u^r_{i,j}$ and $u^*_{i,j}$ represent the pixel values of the restored and original images, respectively.

Table 1. Numerical results of FR and BBS algorithms.

Image	Noise level r (%)	FR-Method			BBS1-Method			BBS2-Method			BBS3-Method		
		NI	NF	PSNR (dB)	NI	NF	PSNR (dB)	NI	NF	PSNR (dB)	NI	NF	PSNR (dB)
Lena	50	82	153	30.5529	56.0	111.0	30.4724	56.0	104.0	30.4796	55.0	109.0	30.4236
	70	81	155	27.4824	54.0	107.0	27.3762	57.0	107.0	27.3194	55.0	107.0	27.4731
	90	108	211	22.8583	52.0	103.0	22.977	56.0	103.0	22.9068	68.0	133.0	22.9178
House	50	52	53	30.6845	37.0	74.0	34.655	35.0	67.0	34.9789	39.0	74.0	34.7593
	70	63	116	31.2564	42.0	83.0	30.8544	43.0	84.0	31.1078	43.0	83.0	30.6449
	90	111	214	25.287	51.0	99.0	25.0459	53.0	101.0	24.8747	49.0	97.0	24.8855
Elaine	50	35	36	33.9129	29.0	56.0	33.889	28.0	50.0	33.843	29.0	53.0	33.8275
	70	38	39	31.864	32.0	61.0	31.8496	33.0	59.0	31.8269	34.0	63.0	31.8462
	90	65	114	28.2019	42.0	81.0	28.0959	41.0	77.0	28.236	42.0	79.0	28.2479
Cameraman	50	59	87	35.5359	34.0	68.0	35.2873	37.0	73.0	35.5787	36.0	72.0	35.1639
	70	78	142	30.6259	39.0	79.0	30.719	39.0	77.0	30.8041	40.0	80.0	30.8458
	90	121	236	24.3962	50.0	101.0	24.9649	49.0	97.0	24.9709	49.0	98.0	24.6395

Table 1 shows that the proposed algorithms perform better than the FR approach in terms of peak signal to noise ratio, number of iterations, and function evaluations [24].

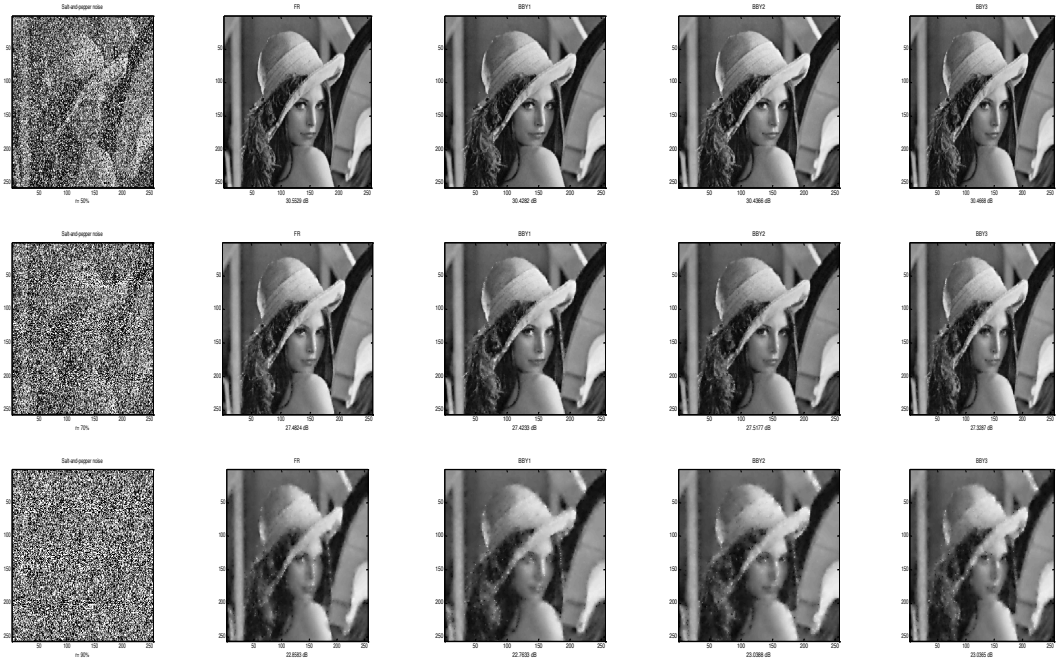

Figure 1. Image restoration results showing original, noisy, and restored images using different methods.

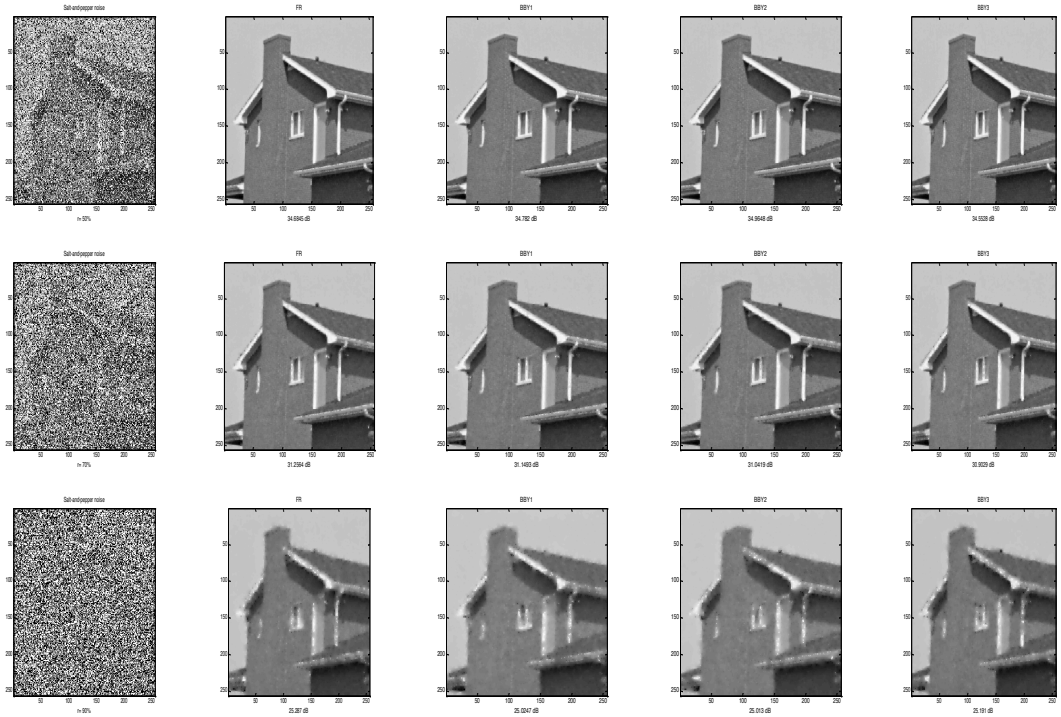

Figure 2. Demonstrates the results of algorithms FR, BBY1, BBY2 and BBY3 of 256 × 256 House image

Figure 3. Demonstrates the results of algorithms FR, BBY11, BBY2 and BBY3 of 256 × 256 Elaine image.

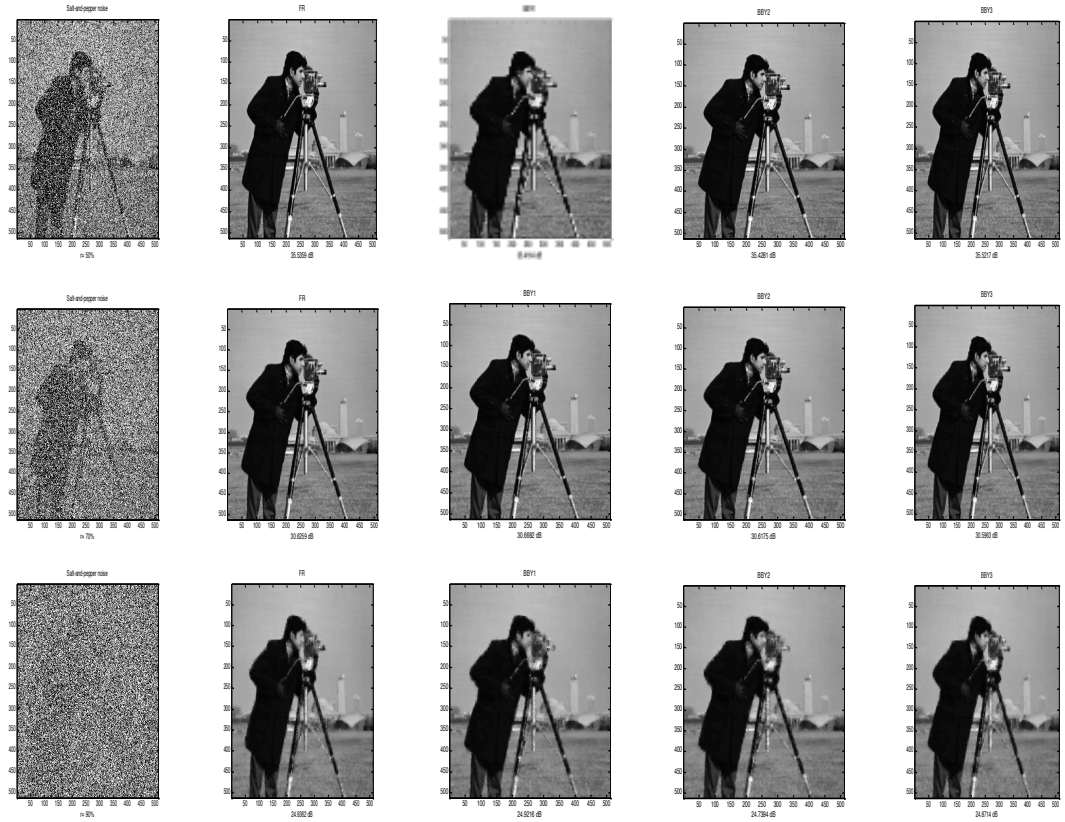

Figure 4. Demonstrates the results of algorithms FR, BBY11, BBY2 and BBY3 of 256 × 256 Cameraman image.

Additionally, a performance profiling approach suggested by Dolan and More [21, 27] was used to assess the results. This technique uses a cumulative distribution function to show how likely it is that a certain algorithm would resolve an issue within a given factor of the highest performance ever noted. The resultant graph displays the performance ratio on the x-axis and the percentage of test cases that were resolved within that ratio on the y-axis. An algorithm is seen more successful if its curve continuously sits above others, indicating that it can answer a higher percentage of problems more quickly.

In terms of the number of iterations (NI) required to achieve convergence, Figure 5 shows the performance profile curve contrasting the suggested approach with the traditional FR technique. The graph shows that the suggested BBS approaches have a better convergence speed and attain greater cumulative performance more quickly [28, 29]. This implies that the suggested approach usually solves most test functions with less iterations. On the other hand, the lagging curve of the classical FR algorithm indicates a slower rate of convergence, which suggests a higher number of iterations and lower computational efficiency.

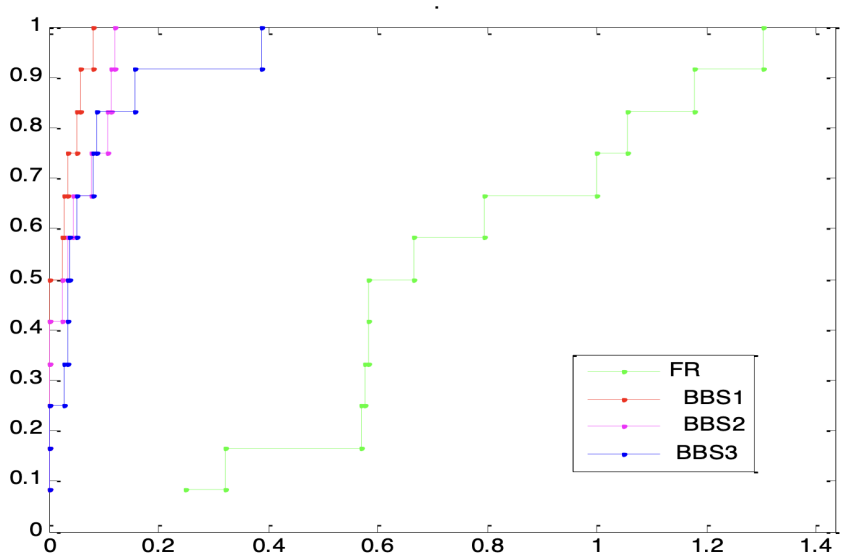

Figure 5. Performance on the number of iterations.

Ultimately, the function evaluation results displayed in Figure 6 highlight how important function evaluations are in determining an optimization algorithm's total computing cost. Because the green line, which represents the standard FR algorithm, is always below the red line, which represents the BBS approaches, the displayed curve further supports the effectiveness of the suggested algorithm. Because of its dominance, the suggested approach often needs fewer function evaluations to arrive at an ideal answer. As function evaluations are frequently the most resource-intensive component of optimization, this result highlights the BBS algorithms' computational advantage over their classical equivalent.

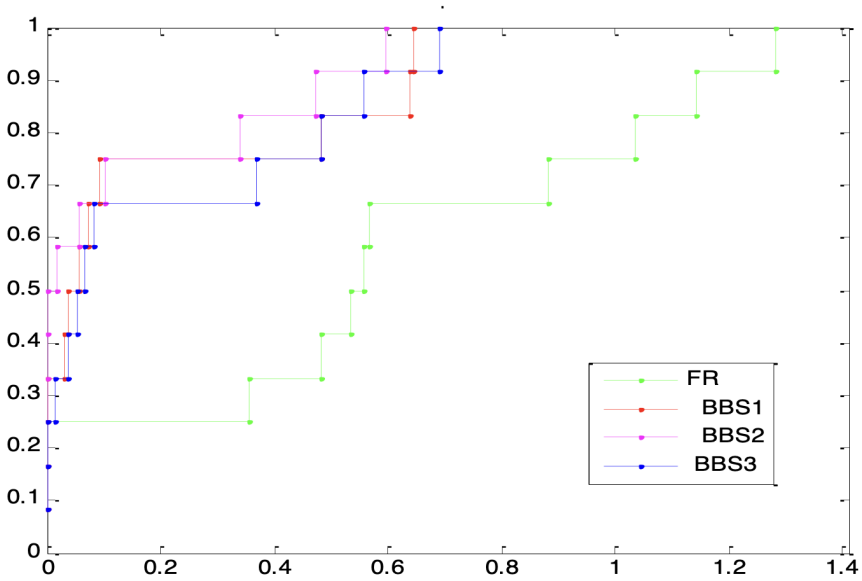

Figure 6. Function evaluations performance.

5. Conclusions

The current work has introduced and tested comprehensively a high-accuracy conjugate gradient (CG) optimization method, the BBS algorithm, for high-fidelity image deblurring of salt-and-pepper noisy images. The proposed approach relies on a two-step procedure: initial noisy pixels are detected and isolated via an adaptive median filter, and then a nonsmooth optimization problem is rearranged into a smooth formulation and solved using the BBS algorithm. The major innovation is the development of a new parameter through Taylor series approximations to maximize computational efficiency and convergence.

Numerical experiments on typical test images (Lena, House, Elaine, Cameraman) demonstrated that BBS algorithm outperforms classical Fletcher-Reeves (FR) algorithm in the aspects of faster convergence, lower computational cost and better restoration quality. Theoretical analysis established the global convergence of BBS algorithm under Lipschitz continuity and descent conditions. Performance profiling also proved its superiority with results indicating that BBS always has solutions with fewer iterations and function evaluations compared to FR. Lastly, the BBS algorithm provides a stable and computationally efficient solution to image restoration, especially in the restoration of salt-and-pepper noise. Its extension to other noise models or integration with deep learning algorithms for further improvement can be considered in future studies.

Authors' Contributions. All authors have read and approved the final version of the manuscript. The authors contributed equally to this work.

Acknowledgment. The Researcher would like to thank the Deanship of Graduate Studies and Scientific Research at Qassim University for financial support (QU-APC-2025).

Conflicts of Interest. The authors declare that there are no conflicts of interest regarding the publication of this paper.

References

[1] B.A. Hassan, H.A. Alashoor, On Image Restoration Problems Using New Conjugate Gradient Methods, Indones. J. Electr. Eng. Comput. Sci. 29 (2023), 1438. https://doi.org/10.11591/ijeecs.v29.i3.pp1438-1445.

[2] B.A. Hassan, H.M. Sadiq, A New Formula on the Conjugate Gradient Method for Removing Impulse Noise Images, Bull. South Ural. State Univ. Ser. Math. Model. Program. Comput. Softw. 15 (2022), 123–130. https://doi.org/10.14529/mmp220412.

[3] H.M. Khudhur, B.A. Hassan, S. Aji, Superior Formula for Gradient Impulse Noise Reduction from Images, Int. J. Appl. Comput. Math. 10 (2023), 4. https://doi.org/10.1007/s40819-023-01637-w.

[4] W. Xue, J. Ren, X. Zheng, Z. Liu, Y. Liang, A New DY Conjugate Gradient Method and Applications to Image Denoising, IEICE Trans. Inf. Syst. E101.D (2018), 2984–2990. https://doi.org/10.1587/transinf.2018EDP7210.

[5] R. Chan, Chung-Wa, M. Nikolova, Salt-And-Pepper Noise Removal by Median-Type Noise Detectors and Detail-Preserving Regularization, IEEE Trans. Image Process. 14 (2005), 1479–1485. https://doi.org/10.1109/tip.2005.852196.

[6] T. Alharbi, A. Ninh, E. Subasi, M.M. Subasi, The Value of Shape Constraints in Discrete Moment Problems: A Review and Extension, Ann. Oper. Res. 318 (2022), 1–31. https://doi.org/10.1007/s10479-022-04789-y.

[7] G. Yu, J. Huang, Y. Zhou, A Descent Spectral Conjugate Gradient Method for Impulse Noise Removal, Appl. Math. Lett. 23 (2010), 555–560. https://doi.org/10.1016/j.aml.2010.01.010.

[8] G. Yu, L. Qi, Y. Sun, Y. Zhou, Impulse Noise Removal by a Nonmonotone Adaptive Gradient Method, Signal Process. 90 (2010), 2891–2897. https://doi.org/10.1016/j.sigpro.2010.04.017.

[9] C. Souli, R. Ziadi, A. Bencherif-Madani, H.M. Khudhur, A Hybrid CG Algorithm for Nonlinear Unconstrained Optimization With Application in Image Restoration, J. Math. Model. 12 (2024), 301–317.

[10] I.H. Halil, I.A. Moghrabi, A.A. Fawze, B.A. Hassan, H.M. Khudhur, A Quadratic Model Based Conjugate Gradient Optimization Method, WSEAS Trans. Math. 22 (2023), 925–930. https://doi.org/10.37394/23206.2023.22.101.

[11] J. Nocedal, S.J. Wright, Numerical Optimization, Springer New York, 2006. https://doi.org/10.1007/978-0-387-40065-5.

[12] P. Wolfe, Convergence Conditions for Ascent Methods, SIAM Rev. 11 (1969), 226–235. https://doi.org/10.1137/1011036.

[13] R. Fletcher, Function Minimization by Conjugate Gradients, Comput. J. 7 (1964), 149–154. https://doi.org/10.1093/comjnl/7.2.149.

[14] L. Nazareth, A Relationship Between the BFGS and Conjugate Gradient Algorithms and Its Implications for New Algorithms, SIAM J. Numer. Anal. 16 (1979), 794–800. https://doi.org/10.1137/0716059.

[15] B.A. Hassan, H. Alashoor, A New Type Coefficient Conjugate on the Gradient Methods for Impulse Noise Removal in Images, Eur. J. Pure Appl. Math. 15 (2022), 2043–2053. https://doi.org/10.29020/nybg.ejpam.v15i4.4579.

[16] B.A. Hassan, H. Sadiq, Efficient New Conjugate Gradient Methods for Removing Impulse Noise Images, Eur. J. Pure Appl. Math. 15 (2022), 2011–2021. https://doi.org/10.29020/nybg.ejpam.v15i4.4568.

[17] B. A. Hassan, A. Ahmed A. Abdullah, Improvement of Conjugate Gradient Methods for Removing Impulse Noise Images, Indones. J. Electr. Eng. Comput. Sci. 29 (2022), 245. https://doi.org/10.11591/ijeecs.v29.i1.pp245-251.

[18] W.W. Hager, H. Zhang, A New Conjugate Gradient Method with Guaranteed Descent and an Efficient Line Search, SIAM J. Optim. 16 (2005), 170–192. https://doi.org/10.1137/030601880.

[19] M.A. Elhamid, H.M. Khudhur, A Globally Convergent of Two Conjugate Gradient Methods with Application to Image Restoration Problems, Numer. Algebr. Control. Optim. 15 (2025), 645–660. https://doi.org/10.3934/naco.2024027.

[20] Y. Dai, J. Han, G. Liu, D. Sun, H. Yin, et al., Convergence Properties of Nonlinear Conjugate Gradient Methods, SIAM J. Optim. 10 (2000), 345–358. https://doi.org/10.1137/s1052623494268443.

[21] E.D. Dolan, J.J. Moré, Benchmarking Optimization Software with Performance Profiles, Math. Program. 91 (2002), 201–213. https://doi.org/10.1007/s101070100263.

[22] M. Großmann, M. Grunert, E. Runge, A Robust, Simple, and Efficient Convergence Workflow for GW Calculations, npj Comput. Mater. 10 (2024), 135. https://doi.org/10.1038/s41524-024-01311-9.

[23] Y. Yang, C. Liu, H. Wu, D. Yu, A Distorted-Image Quality Assessment Algorithm Based on a Sparse Structure and Subjective Perception, Mathematics 12 (2024), 2531. https://doi.org/10.3390/math12162531.

[24] O. Tong, A. Katz, Y. Yanagita, A. Casey, R. Schaap, High-Order Methods for Turbulent Flows on Three-Dimensional Strand Grids, J. Sci. Comput. 67 (2015), 84–102. https://doi.org/10.1007/s10915-015-0070-z.

[25] H.M. Khudhur, I.H. Halil, Noise Removal from Images Using the Proposed Three-Term Conjugate Gradient Algorithm, Comput. Res. Model. 16 (2024), 841–853. https://doi.org/10.20537/2076-7633-2024-16-4-841-853.

[26] F. Gholami Bahador, P. Mokhtary, M. Lakestani, Mixed Poisson-Gaussian Noise Reduction Using a Time-Space Fractional Differential Equations, Inf. Sci. 647 (2023), 119417. https://doi.org/10.1016/j.ins.2023.119417.

[27] F.G. Bahador, P. Mokhtary, M. Lakestani, A Fractional Coupled System for Simultaneous Image Denoising and Deblurring, Comput. Math. Appl. 128 (2022), 285–299. https://doi.org/10.1016/j.camwa.2022.10.025.

[28] Z. Mousavi, M. Lakestani, M. Razzaghi, Combined Shearlet Shrinkage and Total Variation Minimization for Image Denoising, Iran. J. Sci. Technol. Trans.: Science 42 (2017), 31–37. https://doi.org/10.1007/s40995-017-0327-5.

[29] B.A. Hassan, T. Alharbi, Optimizing Conjugate Gradient Methods for Image Recovery from Salt and Pepper Noise, J. Stat. Appl. Probab. 14 (2025), 627–636. https://doi.org/10.18576/jsap/140610.